

Fig. 4.96 Flow regime map delineating the temporal state of the vortex flow for $H = 40.0$ mm.

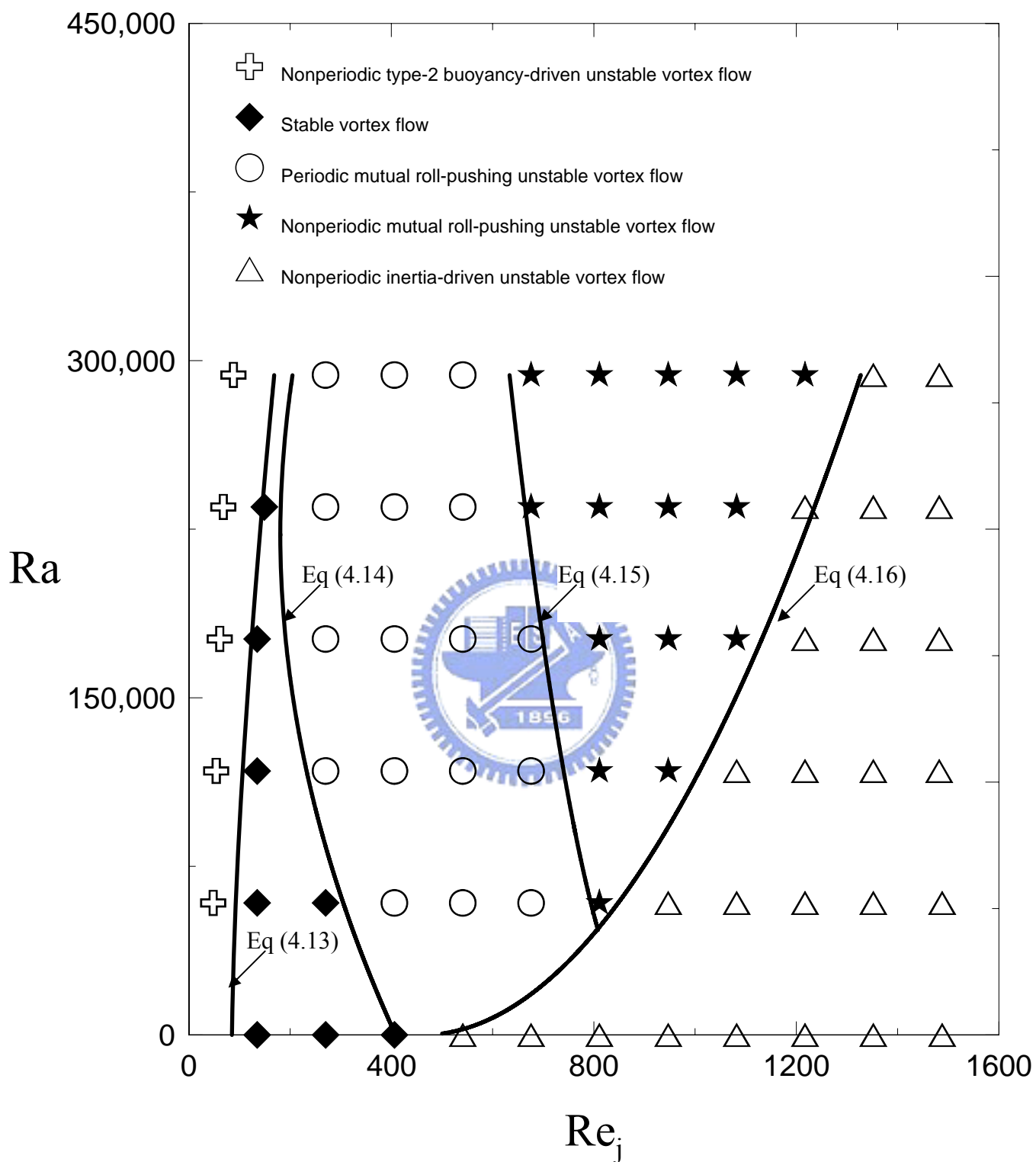


Fig. 4.97 Flow regime map delineating the temporal state of the vortex flow for $H = 50.0$ mm.

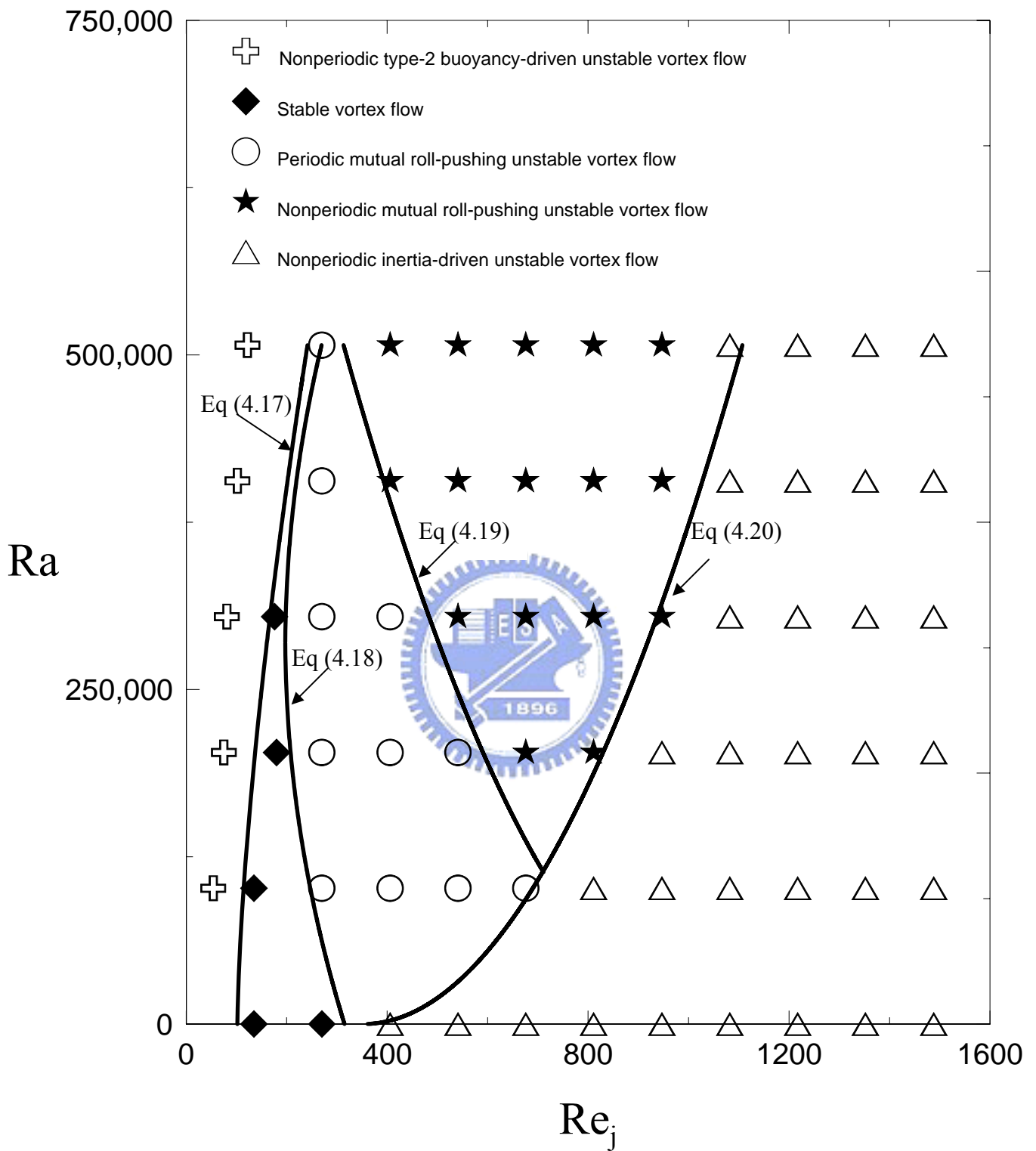


Fig. 4.98 Flow regime map delineating the temporal state of the vortex flow for $H = 60.0$ mm.

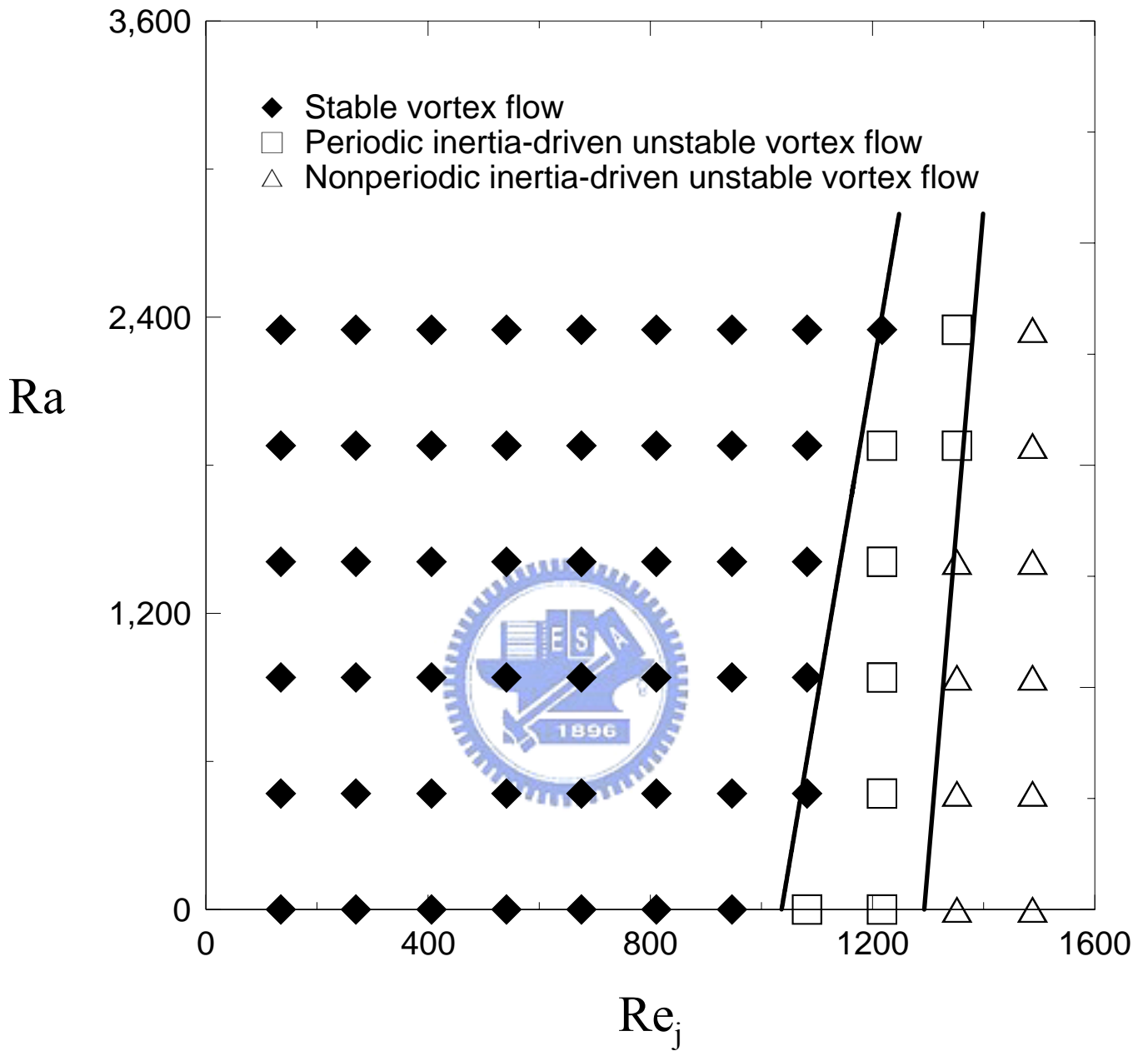


Fig. 4.99 Flow regime map delineating the temporal state of the vortex flow for $H = 10.0$ mm.

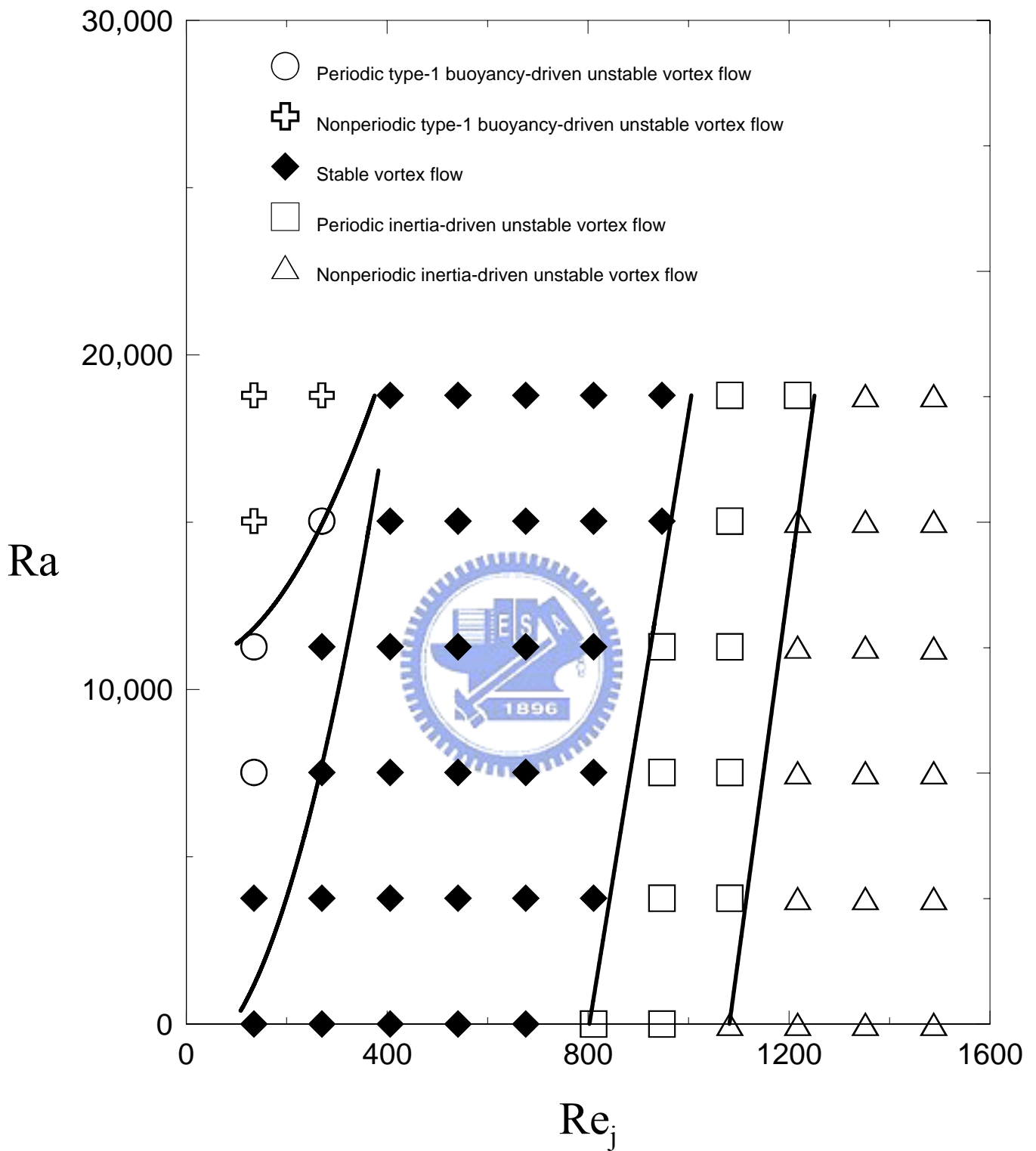


Fig. 4.100 Flow regime map delineating the temporal state of the vortex flow for $H = 20.0$ mm.

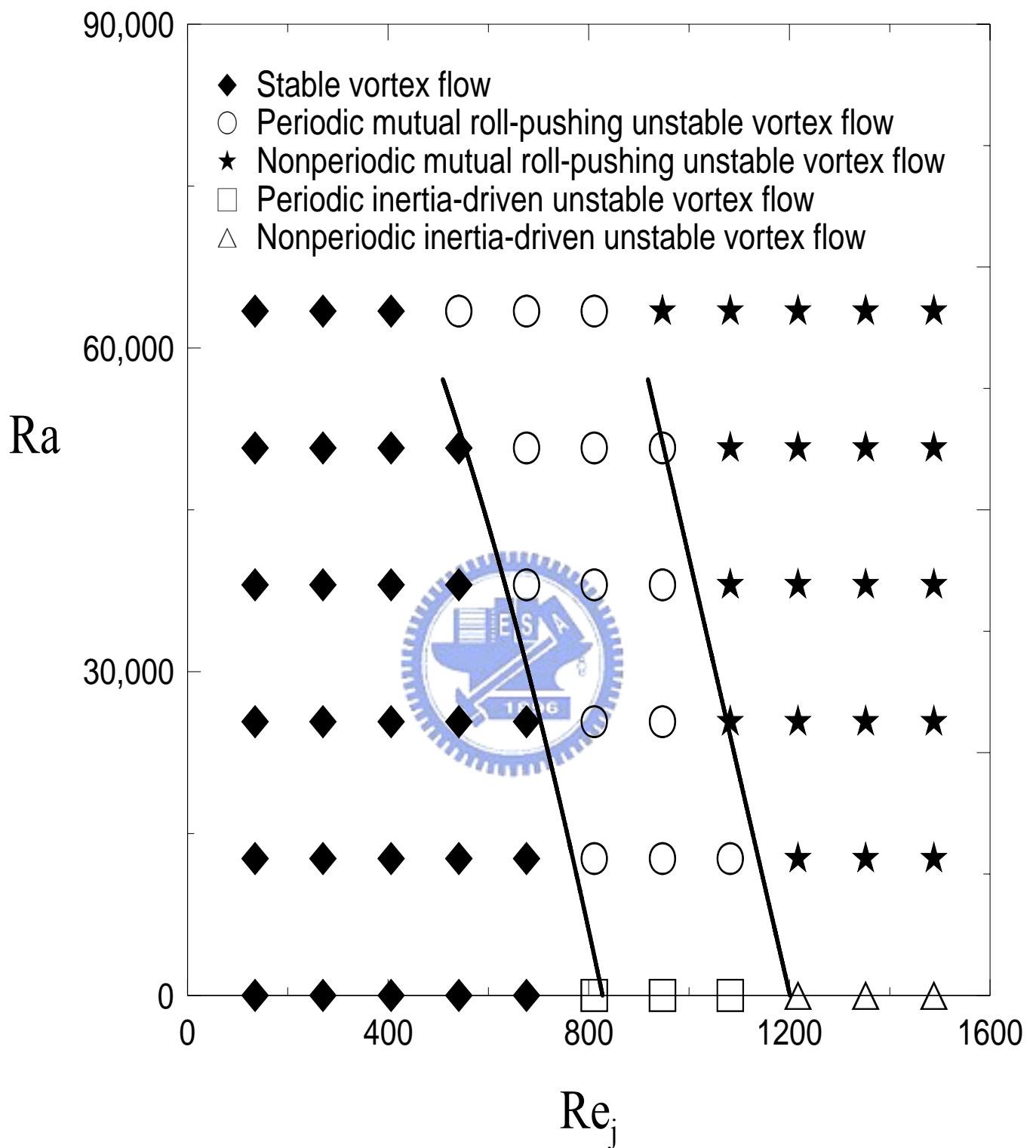


Fig. 4.101 Flow regime map delineating the temporal state of the vortex flow for $H = 30.0$ mm.

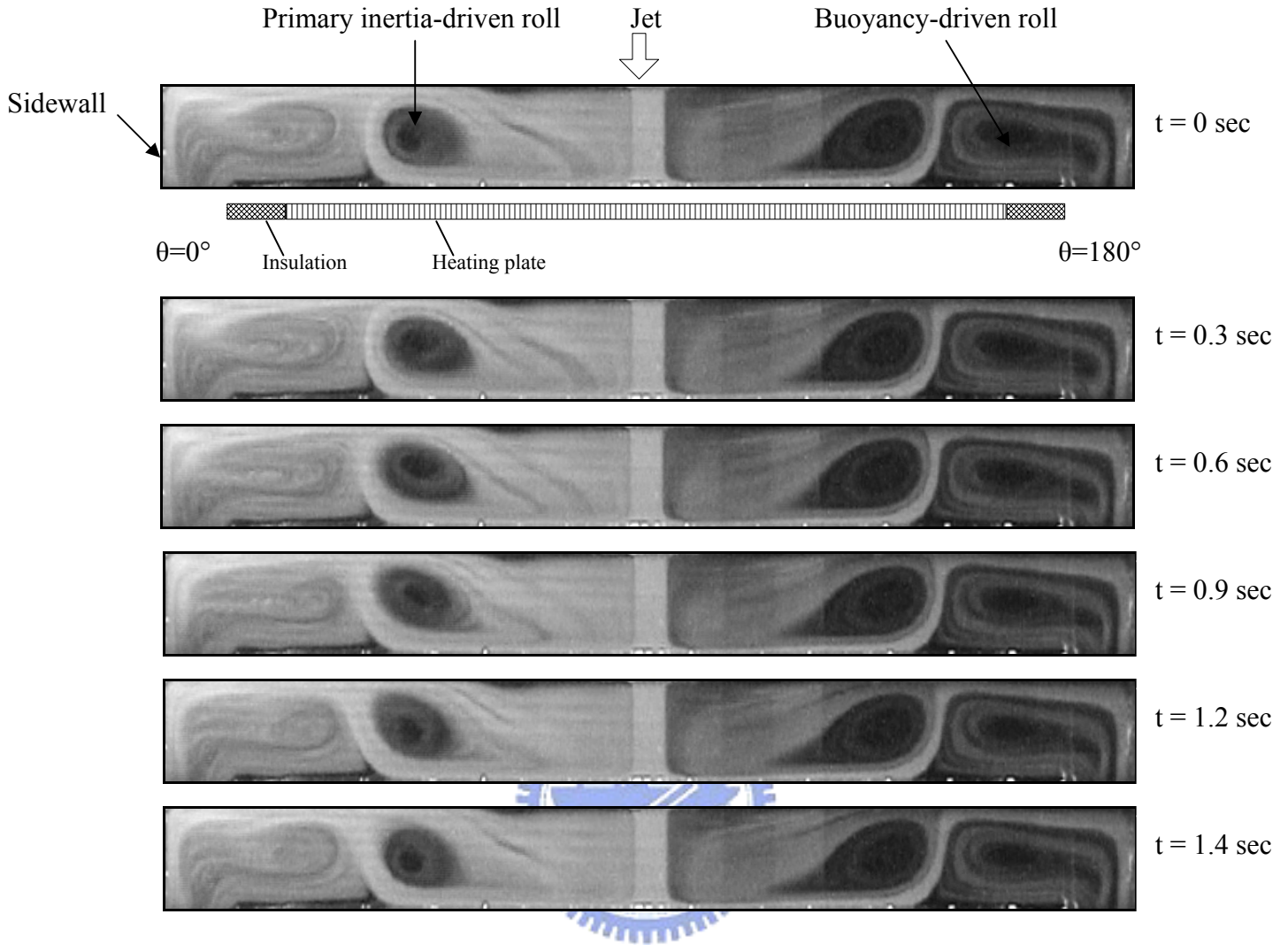


Fig. 4.102 Time-periodic vortex flow for $H = 30.0 \text{ mm}$ and $Ra = 38,051$ ($\Delta T = 15^\circ\text{C}$) at $Re_j = 676$ ($Q_j = 5.0 \text{ slpm}$) illustrated by side view flow photos taken at the cross plane $\theta = 0^\circ$ & 180° at selected time instants in a typical periodic cycle ($t_p = 1.43 \text{ sec}$).

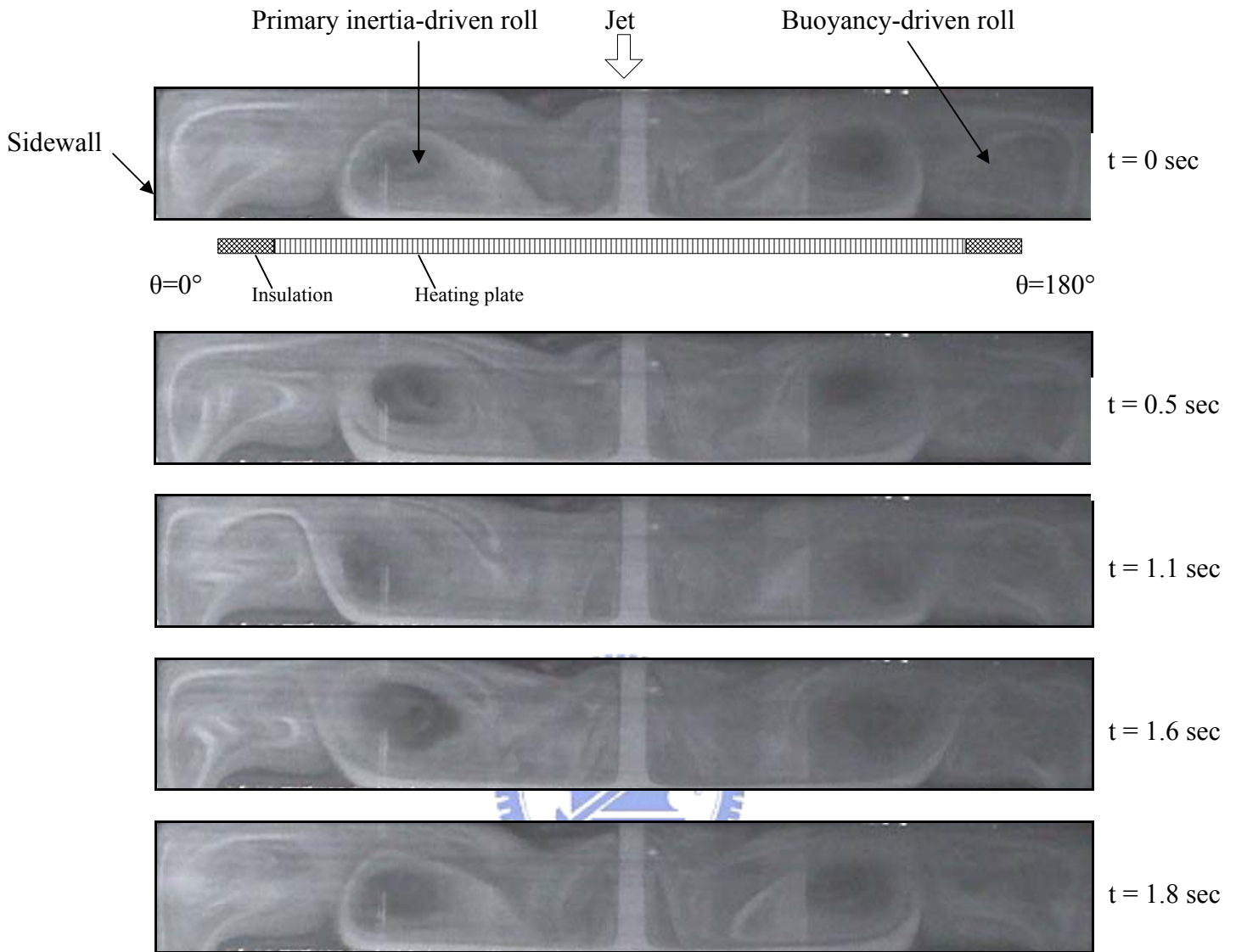


Fig. 4.103 Time-periodic vortex flow for $H = 40.0$ mm and $Ra = 90,195$ ($\Delta T = 15^\circ\text{C}$) at $Re_j = 676$ ($Q_j = 5.0$ slpm) illustrated by side view flow photos taken at the cross plane $\theta = 0^\circ$ & 180° at selected time instants in a typical periodic cycle ($t_p = 1.82$ sec).

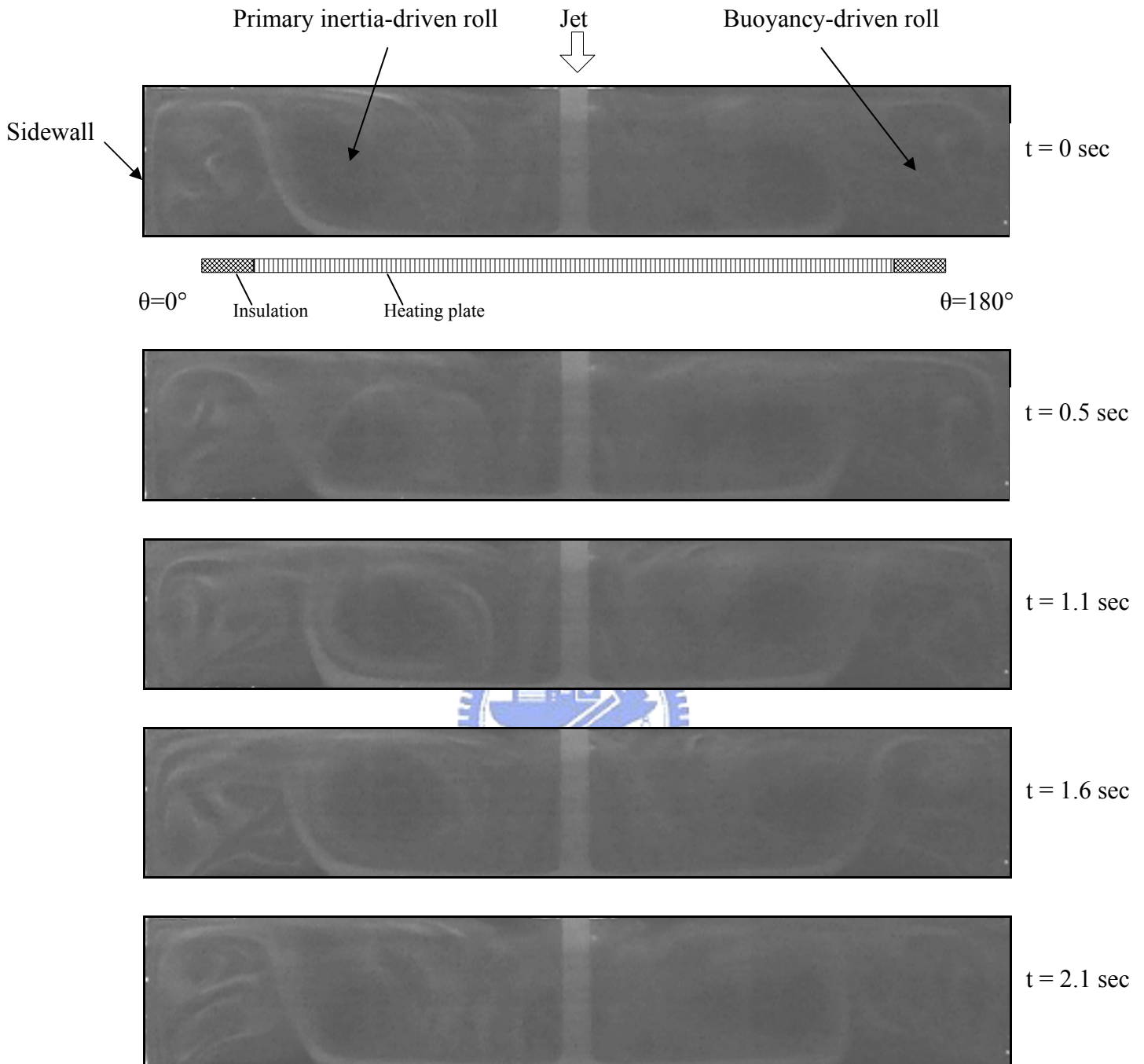


Fig. 4.104 Time-periodic vortex flow for $H = 50.0 \text{ mm}$ and $Ra = 176,162$ ($\Delta T = 15^\circ\text{C}$) at $Re_j = 676$ ($Q_j = 5.0 \text{ slpm}$) illustrated by side view flow photos taken at the cross plane $\theta = 0^\circ$ & 180° at selected time instants in a typical periodic cycle ($t_p = 2.17 \text{ sec}$).

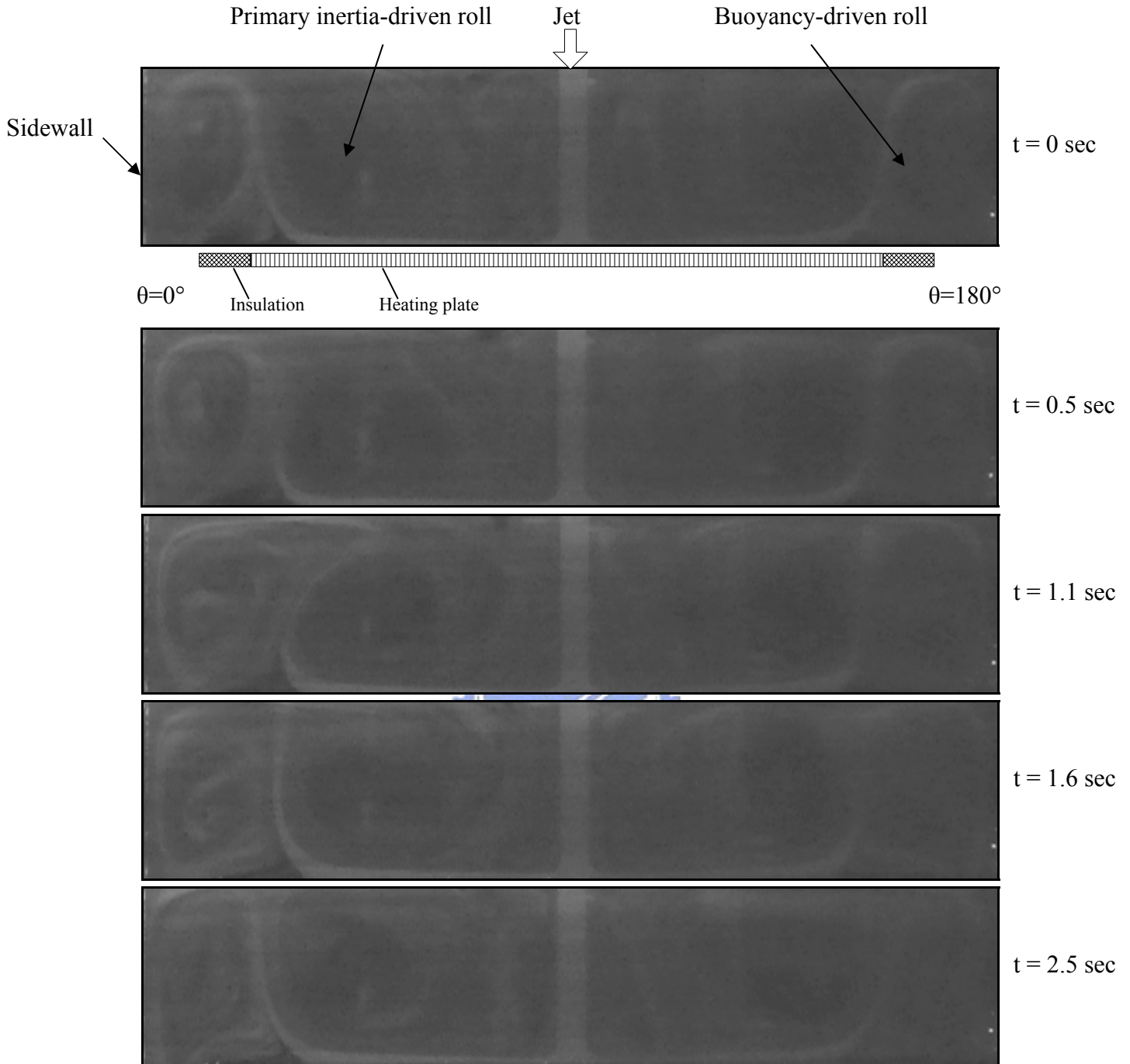


Fig. 4.105 Nonperiodic vortex flow for $H = 60.0$ mm and $Ra = 304,409$ ($\Delta T = 15^\circ\text{C}$) at $Re_j = 676$ ($Q_j = 5.0$ slpm) illustrated by side view flow photos taken at the cross plane $\theta = 0^\circ$ & 180° at selected time instants in a typical periodic cycle.

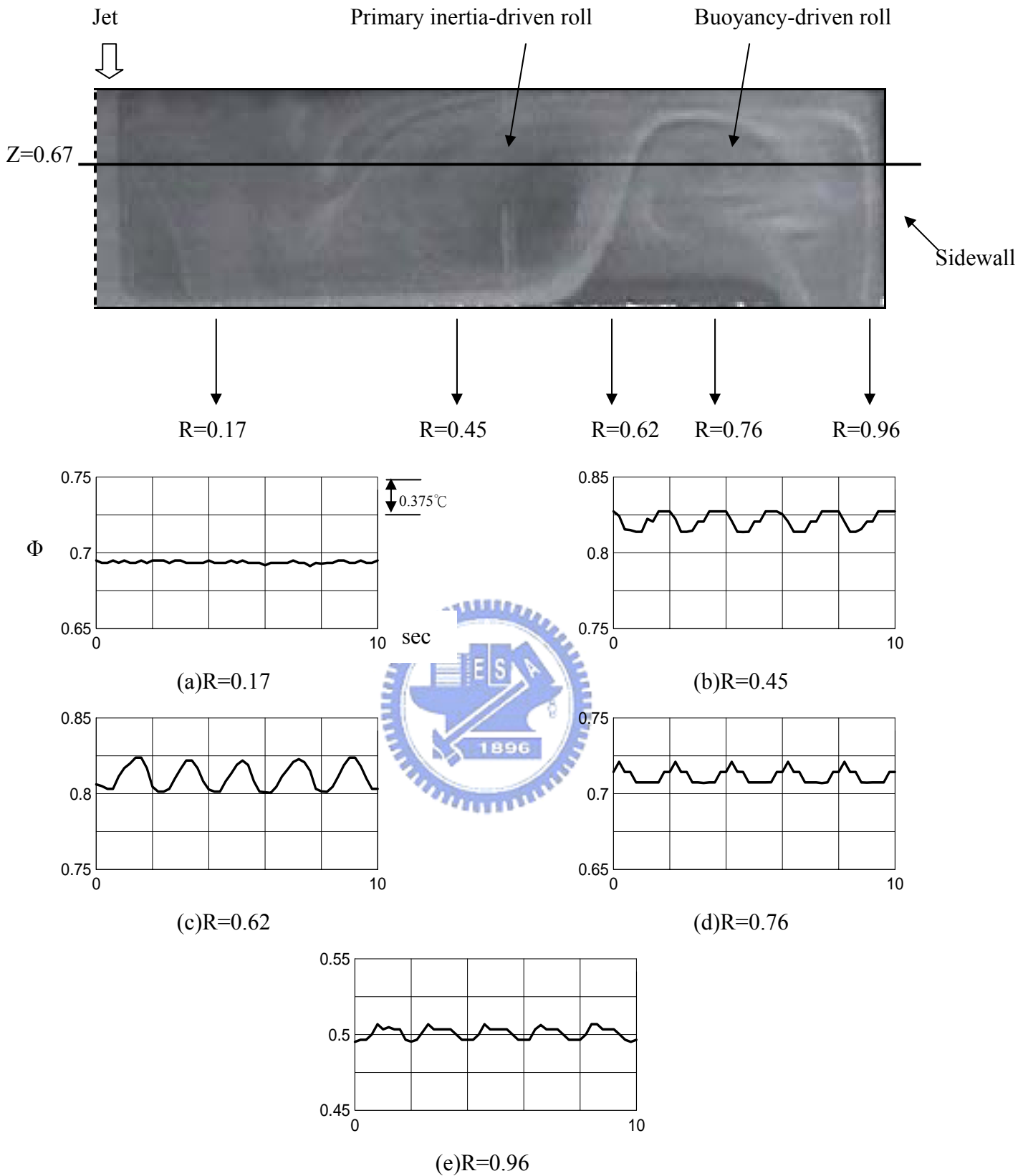


Fig. 4.106 The time records of non-dimensional air temperature for $Ra=90,195$ ($\Delta T = 15.0^\circ C$) and $Re_j=676$ ($Q_j=5.0$ slpm) with $H=40.0$ mm measured at selected locations on the vertical plane $\theta = 0^\circ$ at $Z = 0.67$ for $R = r/R_c =$ (a) 0.17, (b) 0.45, (c) 0.62, (d) 0.76, and (e) 0.96 ($t_p=1.82$ sec).

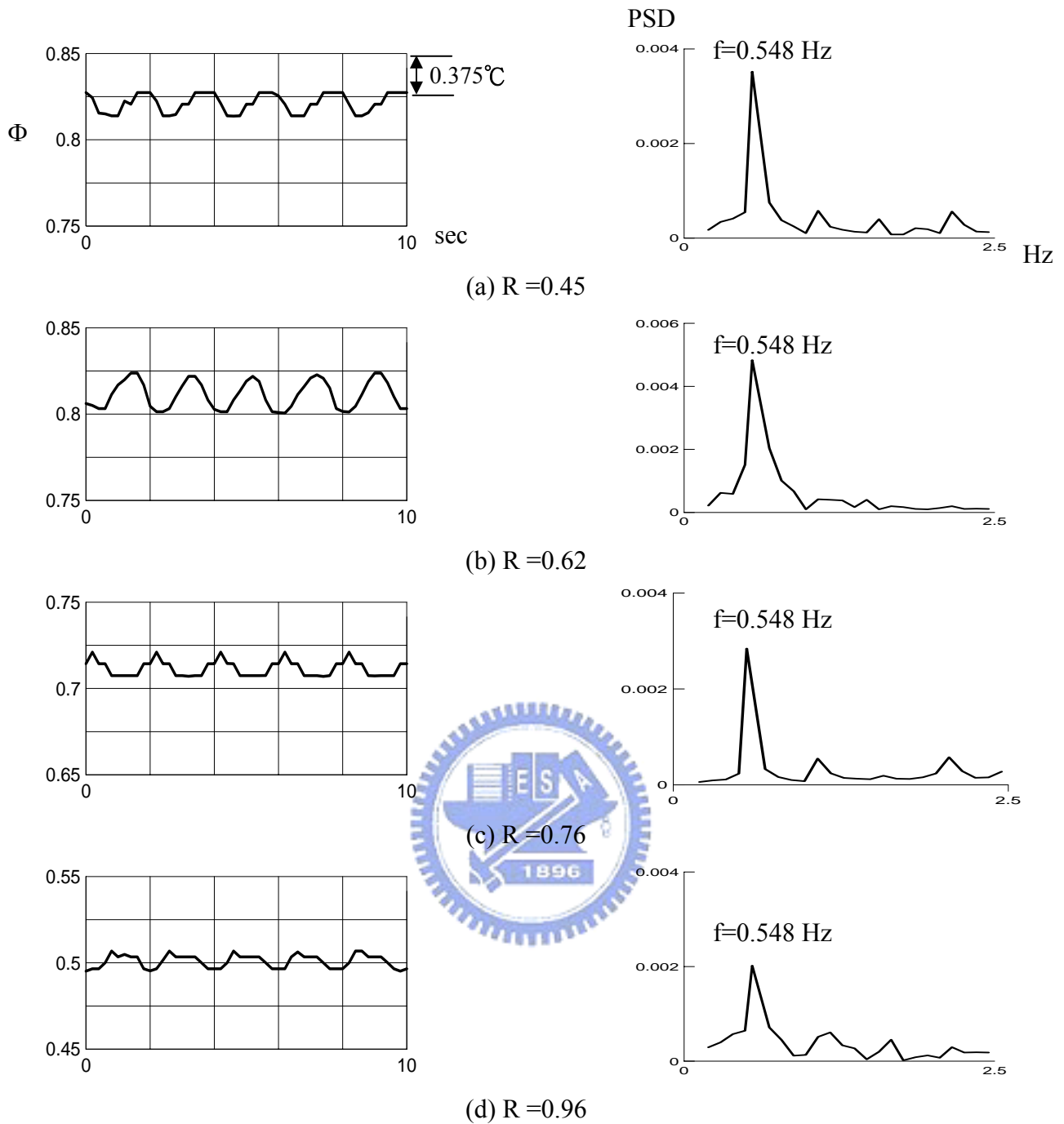


Fig. 4.107 The time records of non-dimensional air temperature and the corresponding power spectrum densities for $Ra=90,195$ ($\Delta T = 15.0^\circ\text{C}$) and $Re_j=676$ ($Q_j=5.0$ slpm) with $H=40.0$ mm measured at selected locations on the vertical plane $\theta = 0^\circ$ at $Z = 0.67$ for $R = r/R_c =$ (a)0.45, (b)0.62, (c)0.76, and (d)0.96 ($t_p=1.82$ sec).

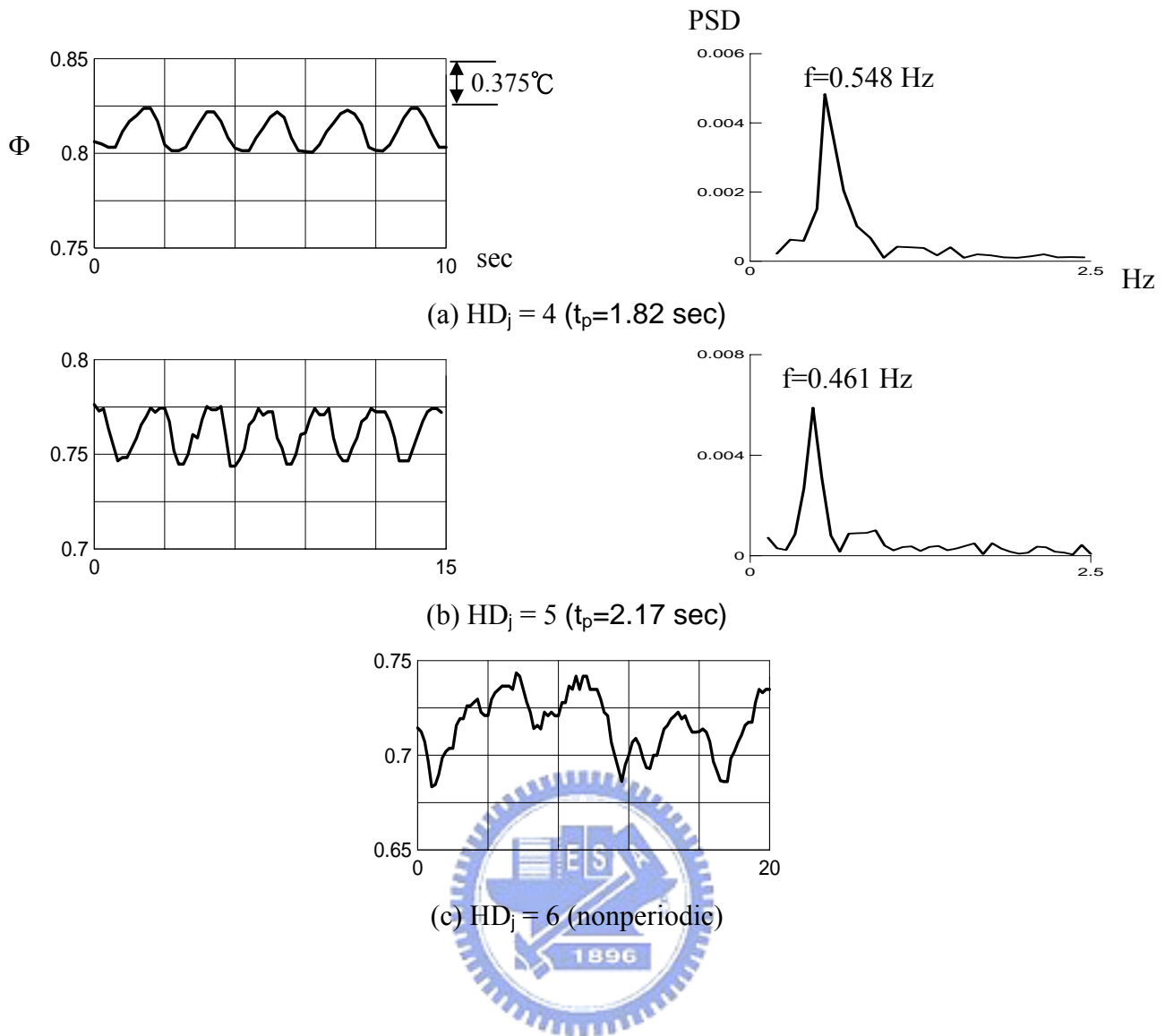


Fig. 4.108 The time records of non-dimensional air temperature and the corresponding power spectrum densities for $\Delta T = 15.0^\circ\text{C}$ and $Re_j = 676$ ($Q_j = 5.0$ slpm) with measured at selected locations on the vertical plane $\theta = 0^\circ$ at $Z = 0.67$ and $R = r/R_c = 0.62$ for various $HD_j =$ (a)4, (b)5, and (c)6.

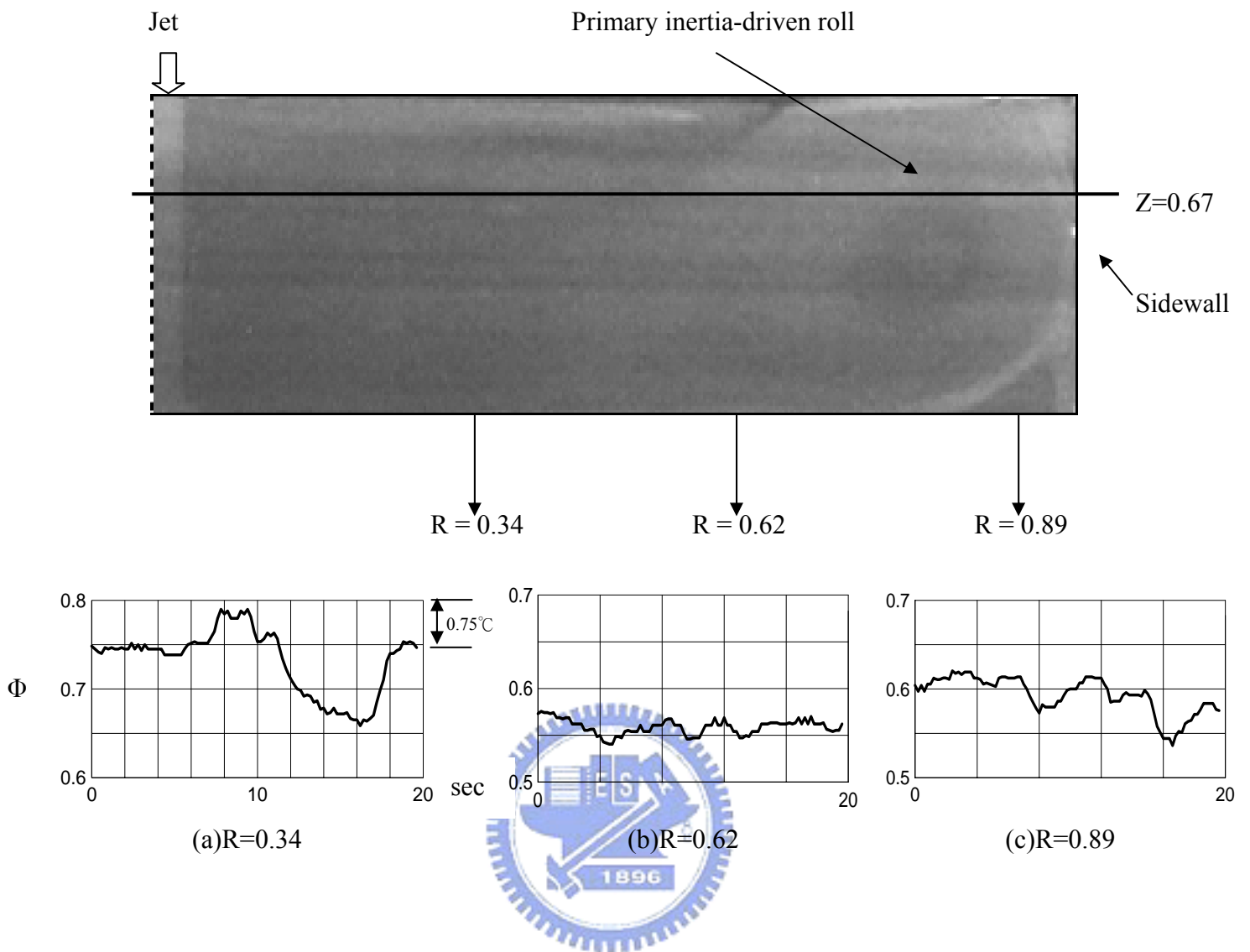


Fig. 4.109 The time records of non-dimensional air temperature for $Ra=176.162$ ($\Delta T = 15.0^\circ C$) and $Re_j=1,488$ ($Q_j=11.0$ slpm) with $H=50.0$ mm measured at selected locations on the vertical plane $\theta = 0^\circ$ at $Z = 0.67$ for $R = r/R_c =$ (a) 0.34, (b) 0.62, and (c) 0.96.

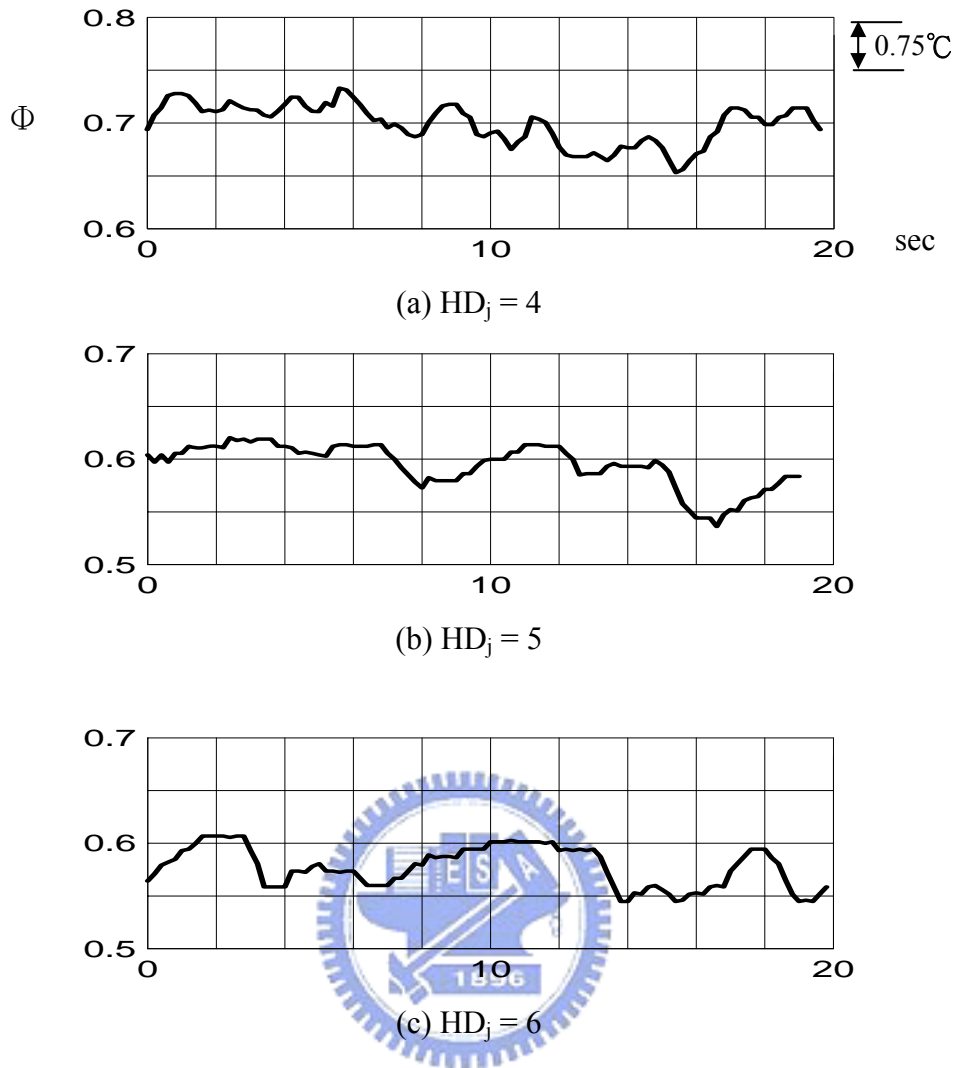


Fig. 4.110 The time records of non-dimensional air temperature for $\Delta T = 15.0^\circ\text{C}$ and $Re_j = 1,488$ ($Q_j = 11.0$ slpm) with measured at selected locations on the vertical plane $\theta = 0^\circ$ at $Z = 0.67$ and $R = r/R_c = 0.62$ for $HD_j =$ (a)4, (b)5, and (c)6.

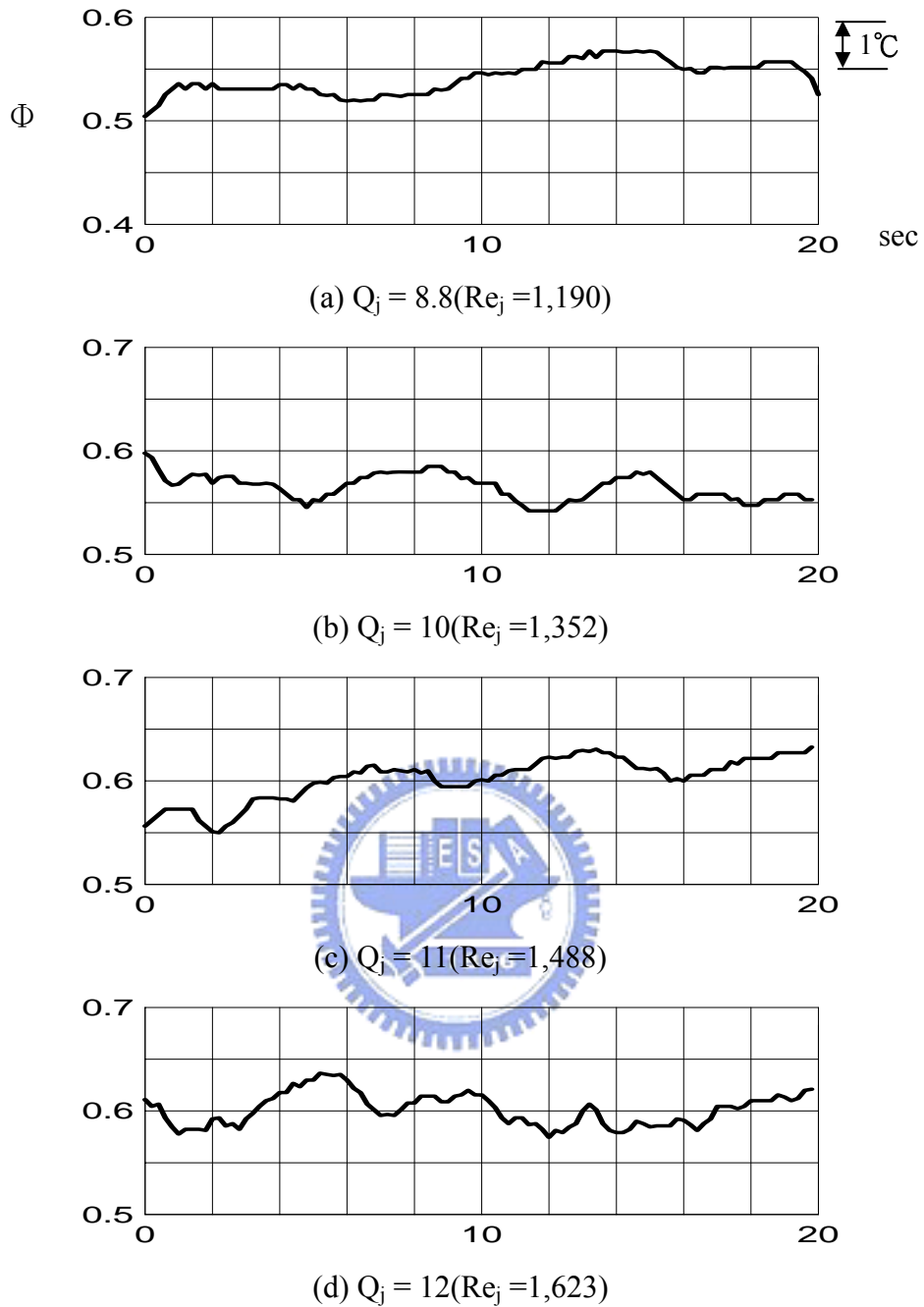


Fig. 4.111 The time records of non-dimensional air temperature for $\Delta T = 20.0^\circ\text{C}$ and $Ra = 234,883$ at $H = 50.0$ mm with measured at selected locations on the vertical plane $\theta = 0^\circ$ at $Z = 0.67$ and $R = r/R_c = 0.89$ for $Re_j =$ (a) 1,190, (b) 1,352, (c) 1,488, and (d) 1,623.

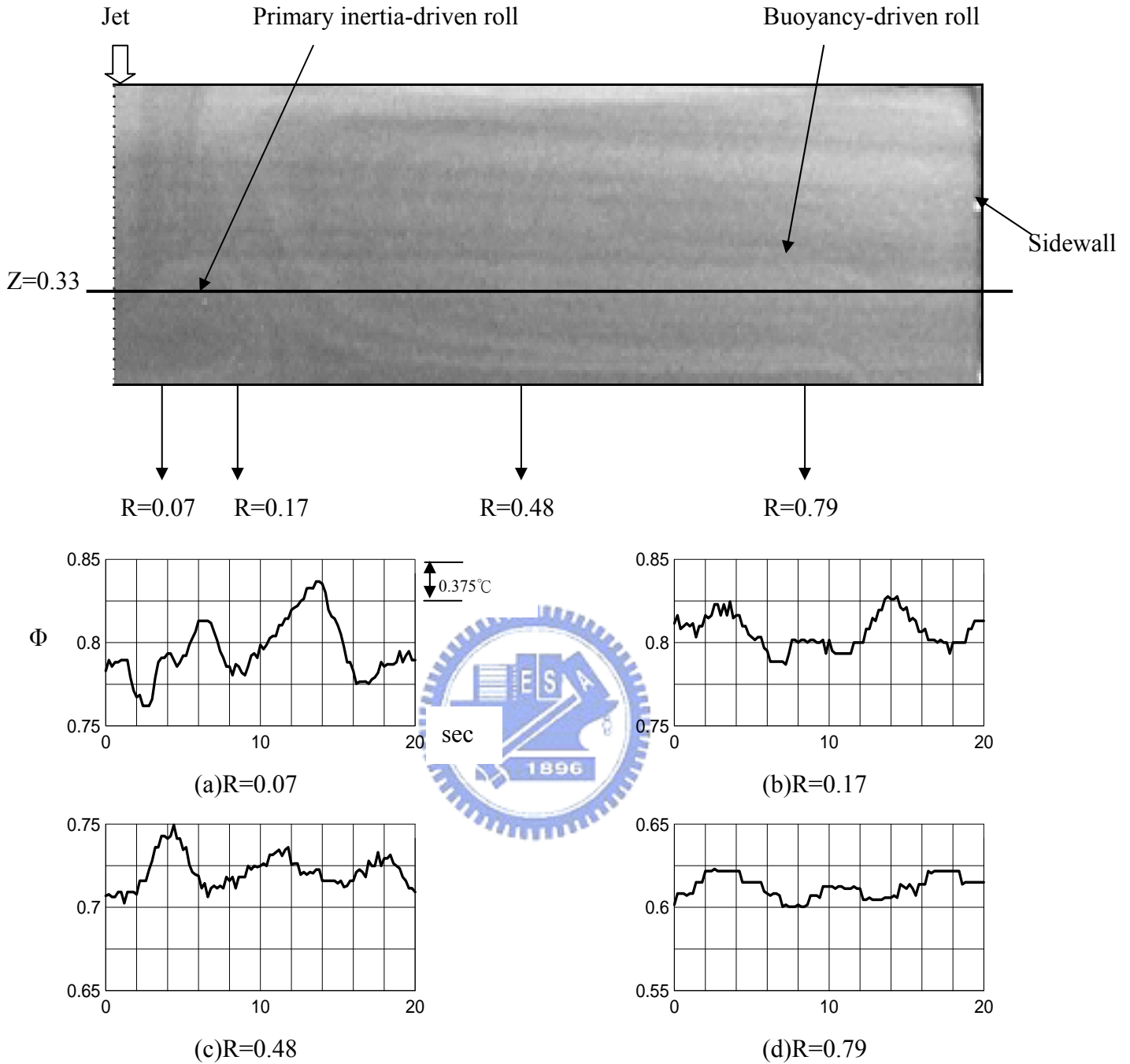


Fig. 4.112 The time records of non-dimensional air temperature for $Ra=176,162$ ($\Delta T = 15.0^\circ\text{C}$) and $Re_j=47$ ($Q_j=0.3$ slpm) with $H=50.0$ mm measured at selected locations on the vertical plane $\theta = 0^\circ$ at $Z = 0.33$ for various $R = r/R_c =$ (a) 0.07, (b) 0.17, (c) 0.48, and (d) 0.79.

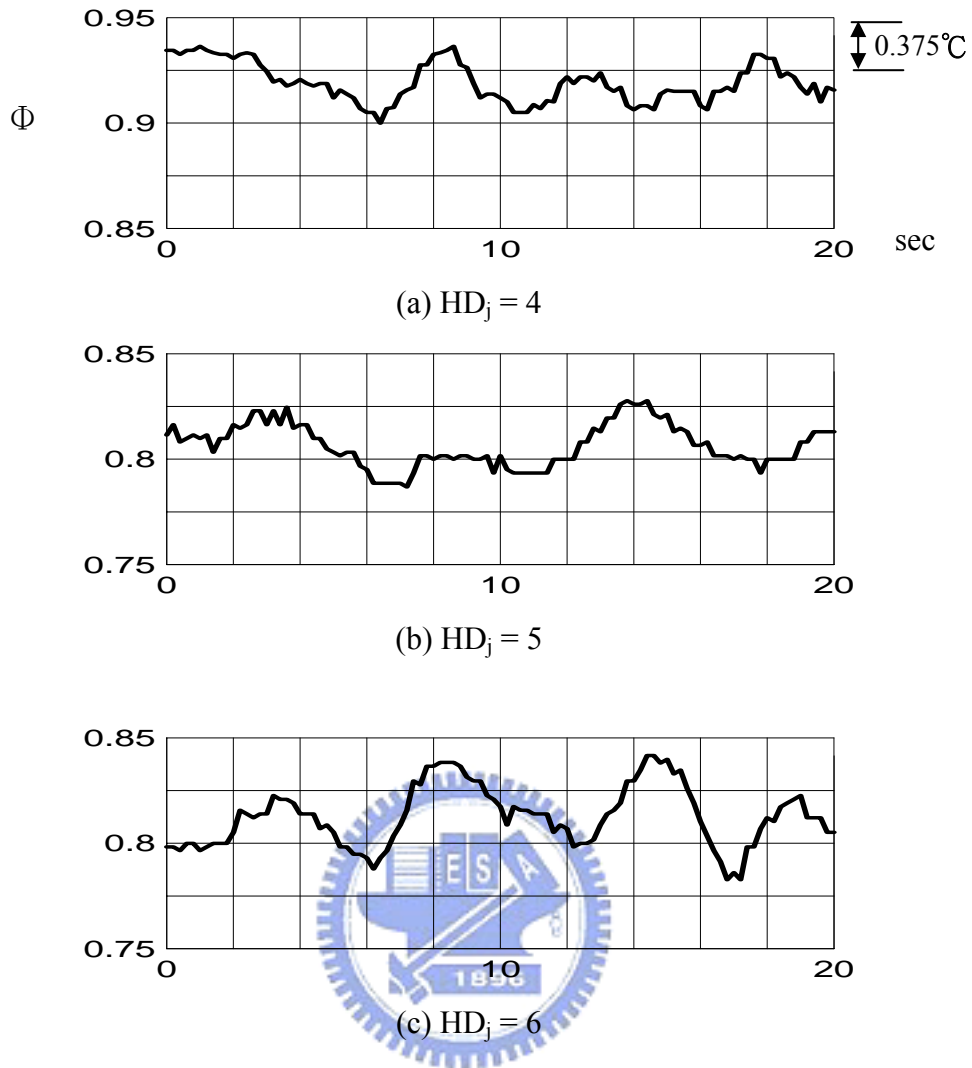
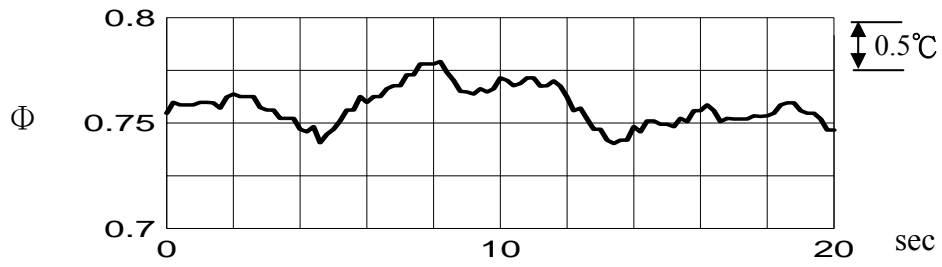
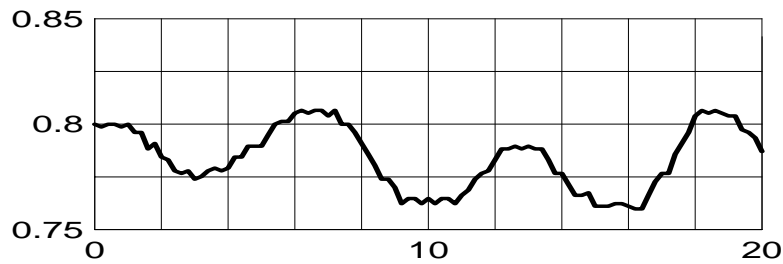


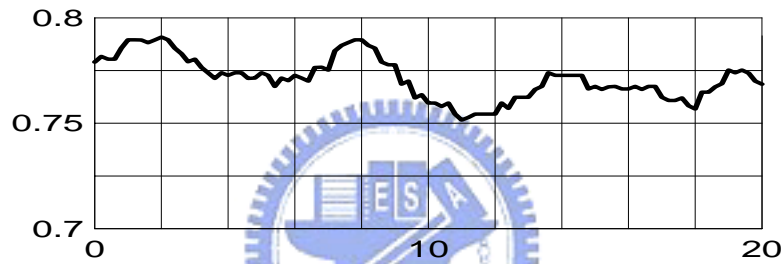
Fig. 4.113 The time records of non-dimensional air temperature for $\Delta T = 15.0^\circ\text{C}$ and $Re_j = 47 (Q_j = 0.3 \text{ slpm})$ with measured at selected locations on the vertical plane $\theta = 0^\circ$ at $Z = 0.33$ and $R = r/R_c = 0.17$ for $HD_j =$ (a)4, (b)5, and (c)6.



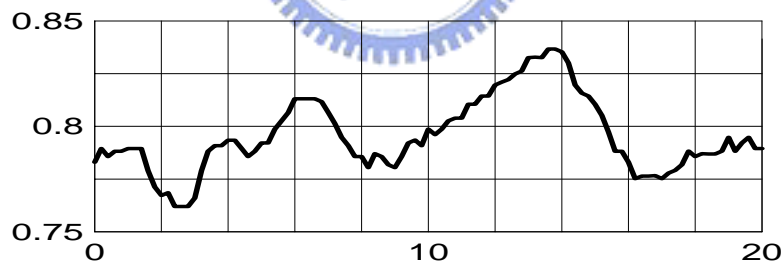
(a) $Q_j = 1 \text{ slpm} (Re_j = 135)$



(b) $Q_j = 0.8 \text{ slpm} (Re_j = 108)$



(c) $Q_j = 0.5 \text{ slpm} (Re_j = 68)$



(d) $Q_j = 0.2 \text{ slpm} (Re_j = 27)$

Fig. 4.114 The time records of non-dimensional air temperature for $\Delta T = 20.0^\circ\text{C}$ and $Ra = 234,883$ at $H = 50.0 \text{ mm}$ with measured at selected locations on the vertical plane $\theta = 0^\circ$ at $Z = 0.33$ and $R = r/R_c = 0.17$ for $Re_j =$ (a) 135, (b) 108, (c) 68, and (d) 27.